

How certain are your uncertainties?*

Luke Whitbread¹[0000-0001-9960-5592] and
Mark Jenkinson^{1,2}[0000-0001-6043-0166]

¹ School of Computer Science, The University of Adelaide, Australia

² Wellcome Centre for Integrative Neuroimaging, University of Oxford, United Kingdom

Abstract. Having a measure of uncertainty in the output of a deep learning method is useful in several ways, such as in assisting with interpretation of the outputs, helping build confidence with end users, and for improving the training and performance of the networks. Therefore, several different methods have been proposed to capture various types of uncertainty, including epistemic (relating to the model used) and aleatoric (relating to the data) sources, with the most commonly used methods for estimating these being test-time dropout for epistemic uncertainty and test-time augmentation for aleatoric uncertainty. However, these methods are parameterised (e.g. amount of dropout or type and level of augmentation) and so there is a whole range of possible uncertainties that could be calculated, even with a fixed network and dataset. This work investigates the stability of these uncertainty measurements, in terms of both magnitude and spatial pattern. In experiments using the well characterised BraTS challenge, we demonstrate substantial variability in the magnitude and spatial pattern of these uncertainties, and discuss the implications for interpretability, repeatability and confidence in results.

Keywords: Uncertainties · Stability · Repeatability · Confidence.

1 Introduction

Magnetic resonance imaging (MRI) is often used to acquire structural brain images in both clinical neurology and research settings. It is common practice to produce anatomical segmentations using these images with manual or automated methods to support a number of clinical and research tasks.

While it is fundamental to any segmentation task to optimise overall measures of success (e.g. Dice/F1 scores), the uncertainties associated with image segmentations have become a salient field of enquiry for researchers; to (i) improve the quality and interpretability of structural delineations, and (ii) improve trust when applying automated techniques to clinical practice [1]. To this end, it is essential to have a thorough treatment of uncertainties to understand the range of possible types of uncertainty and how stable they are.

* Supported by The University of Adelaide.

2 Related Work

Researchers have been investigating uncertainties in medical image segmentations throughout the last decade. Uncertainties have been used for a variety of purposes, such as in diagnostics [4] and improving segmentation times [5]. More recently, epistemic and aleatoric sources of uncertainty have been investigated for deep convolutional networks. Here, two key paradigms have emerged; namely, test-time dropout (**TTD**) for measuring model or epistemic uncertainty and test-time augmentation (**TTA**) to measure data or aleatoric uncertainty. Bayesian networks provide a mathematically sound approach to the measurement of epistemic uncertainties, although as the dimensionality of the parameter space increases, computations become intractable [7,1]. Alternatively, Gal and Ghahramani proposed the use of Monte Carlo dropout at test-time as an approximation to Bayesian model uncertainty, demonstrating its relationship to a deep Gaussian process [7]. Various other methods of approximating model uncertainty have been proposed including Monte Carlo batch normalisation [8] and Markov Chain Monte Carlo methods [9], although use of TTD has garnered widespread use among researchers. In order to measure aleatoric uncertainties, Ayhan and Berens proposed the use of TTA in order to explore data localities [10]. Wang and colleagues further explored the use of TTA, providing a systematic approach to assess aleatoric uncertainties in medical imaging [11]. Building upon these paradigms, research attention has now turned to the incorporation of uncertainties to improve model performance [12,13,14,15].

As the use of uncertainties in imaging pipelines is becoming increasingly common, it is important to perform explorations to assess how stable and reliable these uncertainty estimates are, and what impact hyper-parameter settings have. Additionally, it is of practical interest to know whether various methods of deriving uncertainty maps lead to similar spatial patterns or not, as this has implications for their use in interpretation and for feeding into sub-networks aimed at improving performance. These are the questions driving this work.

3 Methods

We assess the stability of uncertainty measures for epistemic and aleatoric categories by considering various TTD and TTA parameter settings. The parameter space for assessing epistemic uncertainty with TTD is considerably less complex than that for aleatoric categories using TTA. While there are different approaches for how dropout is applied structurally to a model, once this is determined, the key variable is the probability at which dropout is applied. To contrast this with TTA, there are not only a number of augmentation types that can be applied (some of particular relevance to MRI analyses), but there are also typically a number of parameter settings for each augmentation applied.

3.1 Epistemic Uncertainties with TTD

We used the common approach of dropping network filters with a constant global probability. Although researchers sometimes use higher probability parameters at the encoder-decoder junction of a U-net based network, we took the approach of a single probability setting, which still tends to drop more filters at the encoder-decoder junction, given the increasing number of filters with depth.

We have selected 6 TTD probabilities to evaluate the stability of epistemic uncertainties: 0.03, 0.06, 0.09, 0.12, 0.15, and 0.40. The first 5 cases assess uncertainties across a range of typical network-wide dropout settings; while the final setting is intended to test what happens when this is pushed to extremes.

3.2 Aleatoric Uncertainties using TTA

To evaluate the stability of aleatoric uncertainties, we have used 8 TTA cases across three categories common for MRI data: affine transformations (reflecting varying subject orientation), image ghosting and bias-field transforms (both common MRI artefacts). For each category, low and high range parameters have been selected, where the final two cases are transforms composed of all three low or all three high cases. The low settings represent values that would be very likely in practice, whilst the high range settings represent uncommon but plausible values.

Affine transformation cases include the following settings:

- Scaling range: Low = [0.98, 1.02]; High = [0.80, 1.20].
- Rotation degrees: Low = [-5, 5]; High = [-45, 45].
- Image translation (mm): [-5, 5] for both cases.

Ghosting artefacts are a common artefact in MRI data acquisition, usually caused by subject motion in structural scans. This is simulated with settings:

- Intensity strength (max of k-space): Low = [0.0, 0.15]; High = [0.25, 0.75].
- Number of ghosts: [2, 6] for both cases, applied along the 2nd image axis.

Bias-field artefacts result from RF inhomogeneities, manifesting in low-spatial-frequency variations in image intensities. This is simulated as follows:

- Maximum polynomial coefficients: Low = 0.2; High = 0.8
- Polynomial order: 3 for both cases.

3.3 Dataset

This work utilises the well characterised Multimodal Brain Tumor Segmentation (BraTS) 2020 data [16,17,18]. We split the 369 publicly available samples into a hold-out test-set of 78 subjects, a validation-set of 42 subjects, and a training-set of 249 subjects. All contain both high-grade and low-grade glioma cases.

3.4 Experiments and Uncertainty Measures

We have trained a vanilla U-net that produces segmentations for each tumor class (i.e. whole tumor, tumor core, and enhancing tumor). For each TTD and TTA case (as detailed in sections 3.1 and 3.2), each test-set sample is evaluated to produce voxelwise probabilities (of belonging to each class). Each sample is processed 50 times with random dropout or data augmentation applied on each forward pass, creating separate distributions, in each voxel, for each uncertainty case. From each distribution, the mean, variance and entropy are calculated and stored as voxelwise maps for each uncertainty case.

To assess how stable and repeatable these uncertainty values (e.g. entropy) are, we calculated the median and interquartile range, in each voxel separately, as stable measures should have a small range of values. These robust measures would not be substantially affected by one or two unusual/outlier cases.

In addition, to assess whether the spatial pattern is consistent across different settings we measure the spatial correlation, as it is independent of the global magnitude. This was done for each combination of TTD and TTA cases by calculating the correlation coefficients of uncertainty spatial maps, within a mask, for each subject, since the tumor shape and location varies with each subject and so we cannot mix spatial maps across subjects. The spatial mask consisted of all voxels with a non-zero median entropy value (across all cases), thereby excluding a large number of background voxels that otherwise would inflate correlation values. These values produce a correlation matrix for each subject. Additionally, we also calculated the mean of these matrices across subjects, allowing us to assess the consistency of the spatial patterns of different uncertainty maps derived from the network under varying perturbation regimes.

Finally, to assess the overall magnitude of the uncertainty values, independently of the spatial pattern, we have calculated the mean of non-zero uncertainty (e.g. entropy) values by subject for each case, to demonstrate the average level of the uncertainty values exhibited by the network.

4 Results

For brevity, we report results only for tumor core tissue using voxelwise entropy values as our measure of uncertainty. These results generalise to using the variance as the uncertainty measure, as well as to other tumor tissue categories.

4.1 Voxelwise Uncertainty with TTD/TTA Parameter Variations

Figure 1 provides examples of individual entropy maps for all uncertainty cases, as well as the median and interquartile range, in a randomly selected test subject (ID: 197). Across the TTD/TTA parameter settings, it is clear that median entropy levels are reasonably consistent, as we would want them to be. Perhaps more interesting is the interquartile range, where it is clear that even with moderate parameter settings, there is a substantial spread of values in many locations.

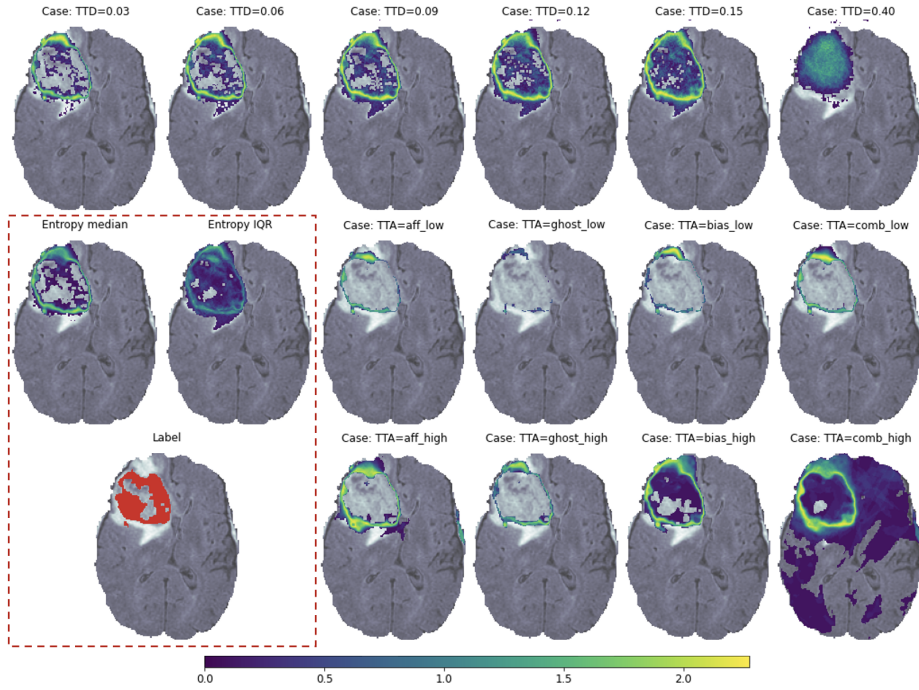


Fig. 1. Subject 197: entropy (uncertainty) maps for different TTD/TTA cases (see sections 3.1 and 3.2), along with the median and interquartile range across all uncertainty cases and the ground truth label in the red highlight box.

4.2 Spatial Correlations

Matrices of spatial correlation between uncertainty cases are shown in figure 2. These allow us to review the similarity of spatial patterns and capture information that is independent of the location and size of tumors. Hence the correlation matrices can be averaged across subjects, to determine whether high and low uncertainty regions are consistently placed.

It can be seen from these results that there are clear similarities among the first 5 TTD cases, although the correlation values reduce as probability settings diverge. A striking result is the negative and near-zero correlation exhibited between case 6 (TTD probability of 0.40) and each of the other TTD and TTA cases. Case 6 provides significant disruption to the network such that non-zero uncertainty values are spread across the whole image (including non-brain regions). Correlations between TTA cases are more varied with a less discernible pattern. This is not unexpected given the variety of data manipulations that are possible using various techniques. Finally, correlations between TTD and TTA cases show a discernible, repeatable pattern, with correlation dropping as the TTD probability parameter is increased; signifying that while low probability TTD cases have similar patterns to aleatoric cases, as this probability increases

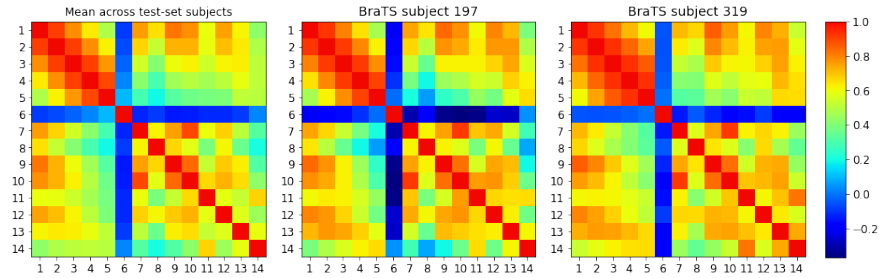


Fig. 2. Correlation matrices (of spatial correlations) for the entropy maps generated from the different TTD and TTA uncertainty cases. The first is the mean across all test subjects, while the others are individual subjects (IDs: 197 and 319). Rows and columns represent the different uncertainty cases in the following order: Cases 1–6: epistemic TTD probability = [0.03, 0.06, 0.09, 0.12, 0.15, 0.40] respectively; Cases 7–14 aleatoric TTA = [7: affine low, 8: ghosting low, 9: bias-field low, 10: combined (affine, ghosting, bias-field) low, 11: affine high, 12: ghosting high, 13: bias-field high, 14: combined (affine, ghosting, bias-field) high]. Specific TTA parameters are detailed in section 3.2.

the spatial pattern of high and low uncertainty regions for these estimates of epistemic and aleatoric uncertainty become increasingly different.

A principal component analysis was also performed across cases for each subject, and then averaged over subjects. This showed that the explained variance of the first principal component was $65.9 \pm 5.9\%$. Across the first three principal components, the explained variance was $85.9 \pm 2.9\%$.

4.3 Mean Uncertainty Levels

Since the spatial correlations are invariant to the global magnitude of the uncertainties, we have also measured the mean of non-zero voxel entropy values for each subject, for each uncertainty case, to quantify global magnitude. These results can be seen in figure 3. Once again, the extreme TTD case (i.e. case 6) is a conspicuous outlier, with much lower values, caused by many low values that are spread across the image. This provides further confirmation that TTD settings with higher probability values are unlikely to be of use. The remaining 5 TTD cases behave similarly, with the distribution of mean levels widening as dropout probability increases. Amongst the TTA cases, the mean levels of the high bias-field and the high-level combined TTA case show distributions that are lower than the general level of the TTA cases.

5 Discussion and Conclusion

It is clear from these results that the parameter settings for both epistemic (TTD) and aleatoric (TTA) uncertainty estimates have a substantial impact on

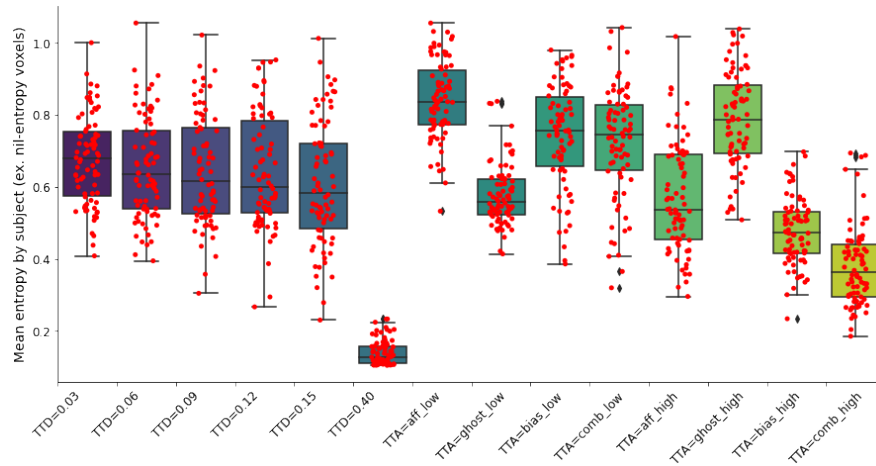


Fig. 3. Boxplots of the spatial mean of non-zero entropy values, taken across subjects, shown separately for each epistemic (TTD) and aleatoric (TTA) uncertainty case. Cases that produce significant network disruption (e.g. case 6 for TTD) can lead to large numbers of voxels with low-level, but non-zero, entropy values.

the uncertainty values generated. Although this is only shown for entropy, it also holds true for variance, and for other tissue classes. We chose to show entropy values mainly because they are better at dealing with distributions that are not unimodal, which we were likely to produce over the range of settings utilised.

In some instances, the interquartile range approached the full range of possible entropy values. This provides a strong indication that the parameters used for TTD or TTA uncertainty estimation are important considerations. For very high dropout rates the TTD uncertainty estimates are clearly not useful for any purpose and, accordingly, researchers must be careful when using dropout settings that lead to network disruption in such significant ways. Furthermore, the calculated uncertainties may gradually change from being useful to non-informative, based on the gradual changes in correlations found at lower dropout values, although further testing would be required to establish this more generally.

Aleatoric uncertainty maps spanned a range of similarities, as shown by the correlation matrices, and this indicates that to generate meaningful aleatoric uncertainties it is likely that a number of different data augmentation types need to be included. In addition, the parameters associated with these augmentations clearly have an effect, and when pushed to higher values can sometimes result in widespread low-grade uncertainties across images. Where this begins to occur, it may be interpreted as a practical upper-bound to parameter settings.

The fact that spatial correlations are moderate to low in many cases, excluding the extreme TTD case, indicates that it is of substantial importance to consider both epistemic and aleatoric uncertainties when performing segmentations.

This is true regardless of whether uncertainties are used to aid interpretability, indicate reliability, or incorporated in uncertainty-aware networks.

Careful consideration of different parameter settings is needed when using TTD and TTA estimation methods, and researchers should consider that “the” uncertainty map is actually a set of different maps that are sensitive to TTD and TTA hyper-parameters. In anthropomorphic terms, TTD reflects how different the output segmentation would be when the network is impaired (e.g. slight inebriation) whilst TTA reflects how different the output segmentation would be when the image is modified (e.g. a visual impairment), whereas what we intuitively think of as “uncertainty” might be more closely related to a self-estimation of error likelihood, which is more difficult to estimate. In order to have reliable, repeatable measures of uncertainty it is important to specify the types of augmentation, and all hyper-parameters, while being able to provide a single uncertainty value or map is even more challenging and may be different for each use case. When using uncertainties in the context of uncertainty-aware networks, it is likely that incorporating more than one map will be beneficial.

In this study the major limitation is the size and nature of the dataset. BraTS is a well studied and characterised dataset, which contains several different segmentation tasks, and thus allowed us to verify that the findings generalised to different tissue types and also different uncertainty measures. However, to establish these results more generally, further studies are required.

In conclusion, we have shown that epistemic and aleatoric uncertainty estimates, as obtained through TTD and TTA respectively, are sensitive to hyper-parameter settings. To obtain repeatable maps it is important to specify the hyper-parameters involved in the estimation methods, and these settings need to be thought through carefully when building and running networks that produce uncertainty estimates. Furthermore, we found that it is important to consider both sources of uncertainty and that there is a richness in the uncertainty estimations that is not captured by a single spatial map, and this should be considered when feeding maps into uncertainty-aware networks or when using them to aid interpretability or indicate reliability. While we found that a large portion of the variance amongst cases could be explained by the first principal component, thus reflecting some similarity in the uncertainty estimates amongst cases, a sizable proportion of the variance ($> 30\%$) is explained by the remaining principal components. This indicates that although a well chosen case may capture uncertainties to some degree, it is unlikely to provide comprehensive estimates across all regions where uncertainties could manifest; which could be vital to ensuring clinical efficacy in challenging situations.

References

1. Dinsdale, N. et. al.: Challenges for machine learning in clinical translation of big data imaging studies. arXiv:2107.05630 (2021)
2. Prassini, J.S. et. al.: Uncertainty-aware guided volume segmentation. In: IEEE Transactions on Visualisation and Computer Graphics **16**(6), pp. 1358–1365 (2010)

3. Saad, A. et. al.: Exploration and visualization of segmentation uncertainty using shape and appearance prior information. In: *IEEE Transactions on Visualisation and Computer Graphics* **16**(6), pp. 1366–1375 (2010)
4. Shi, W. et. al.: A multi-image graph cut approach for cardiac image segmentation and uncertainty estimation. In: Camara, O. et. al. (eds.) *Statistical Atlases and Computational Models of the Heart. Imaging and Modelling Challenges*, 2012, pp. 178–187. Springer, Berlin, Heidelberg (2012)
5. Top, A. et. al.: Active learning for interactive 3D image segmentation. In: Fichtinger, G. et. al. (eds.), *Medical Imaging Computing and Computer Assisted Intervention (MICCAI) 2011*, pp. 603–610. Springer, Berlin, Heidelberg (2011)
6. Al-Taie, A. et. al.: Uncertainty-aware ensemble of classifiers for segmenting brain MRI data. In: *VCBM*, pp. 41–50 (2014)
7. Gal, Y., Ghahramani, Z.: Dropout as a Bayesian approximation: Representing model uncertainty in deep learning. In: *Proceedings of the 33rd International Conference of Machine Learning – vol. 48, ICML’16*, pp. 1050–1059. JMLR.org, (2016)
8. Taye, M., Azizpour, H., Smith, K.: Bayesian uncertainty estimation for batch normalized deep networks. In: *International Conference on Machine Learning*, pp. 4907–4916. PMLR (2018)
9. Neal, R.M.: *Bayesian learning for neural networks*. Springer Science & Business Media (2012)
10. Ayhan, M.S., Berens, P.: Test-time augmentation for estimation of heteroscedastic aleatoric uncertainty in deep neural networks (2018)
11. Wang, G. et. al.: Aleatoric uncertainty estimation with test-time augmentation for medical image segmentation with convolutional neural networks. *Neurocomputing* **338**, pp. 34–34 (2019)
12. Ozdemir, O. et. al.: Propogating uncertainty in multi-stage Bayesian convolutional neural networks with application to pulmonary nodule detection. arXiv:1712.00497 (2017)
13. Herzog, L. et. al.: Integrating uncertainty in deep neural networks for MRI based stroke analysis. In: *Medical Image Analysis* **65**, DOI:10.1016/j.media.2020.101790 (2020)
14. Wang, G. et. al.: Automatic brain tumor segmentation based on cascaded convolutional neural networks with uncertainty estimation. In: *Frontiers in Computational Neuroscience* **13**(56), DOI:10.3389/fncom.2019.00056 (2019)
15. Arega, T.W. et. al.: Leveraging Uncertainty Estimates to Improve Segmentation Performance in Cardiac MR. In: *MICCAI Uncertainty for Safe Utilization of Machine Learning in Medical Imaging (UNSURE), and Perinatal Imaging, Placental and Preterm Image Analysis*, pp. 24–33. Springer, Cham (2021)
16. Menze, A. et. al.: The Multimodal Brain Tumor Image Segmentation Benchmark (BRATS). In: *IEEE Transactions on Medical Imaging* **34**(10), 1993–2024, DOI:10.1109/TMI.2014.2377694 (2015)
17. Bakas, H. et. al.: Advancing the Cancer Genome Atlas glioma MRI collections with expert segmentation labels and radiomic features. In: *Nature Scientific Data* **4**(170117), DOI:10.1038/sdata.2017.117 (2017)
18. Bakas, S. et. al.: Identifying the Best Machine Learning Algorithms for Brain Tumor Segmentation, Progression Assessment, and Overall Survival Prediction in the BRATS Challenge. arXiv:1811.02629 (2018)